# Bridging Nano and Body Area Networks: A Full Architecture for Cardiovascular Health Applications

Rafael Asorey-Cacheda, *Member, IEEE*, Luis M. Correia, *Senior Member, IEEE*, Concepcion Garcia-Pardo, Krzysztof Wojcik, Kenan Turbic, *Member, IEEE*, and Pawel Kulakowski

***Abstract*—Cardiovascular events occurring in the bloodstream are responsible for about 40% of human deaths in developed countries. Motivated by this fact, we present a new global network architecture for a system for the diagnosis and treatment of cardiovascular events, focusing on problems related to pulmonary artery occlusion, i.e., situations of artery blockage by a blood clot. The proposed system is based on bio-sensors for detection of artery blockage and bio-actuators for releasing appropriate medicines, both types of devices being implanted in pulmonary arteries. The system can be used by a person leading an active life and provides bidirectional communication with medical personnel via nano-nodes circulating in the bloodstream constituting an in-body area network. We derive an analytical model for calculating the required number of nano-nodes to detect artery blockage and the probability of activating a bio-actuator. We also analyze the performance of the body area component of the system in terms of path loss and of wireless links budget. Results show that the system can diagnose a blocked artery in about 3 h and that after another 3-h medicines can be released in the exact spot of the artery occlusion, while with current medical practices the average time for diagnosis varies between 5 and 9 days.**

***Index Terms*—Body area networks (BANs), flow-guided nano-networks, Internet of Things (IoT) for health, medical applications, nano-communications, THz communications.**

Manuscript received 22 July 2022; revised 26 September 2022; accepted 9 October 2022. Date of publication 20 October 2022; date of current version 20 February 2023. This work was supported in part by the COST Action INTERACT under Grant CA20120; in part by the Spanish Agency for Research MCIN/AEI/10.13039/501100011033 under Project PID2020-116329GB-C22, Project PID2020-115005RJ-I0, and Project TED2021-129336B-I00; and in part by the Polish Ministry of Science and Higher Education with the Subvention Funds of the Faculty of Computer Science, Electronics and Telecommunications of AGH University. *(Corresponding author: Pawel Kulakowski.)*

Rafael Asorey-Cacheda is with the Department of Information and Communication Technologies, Universidad Politécnica de Cartagena, 30202 Cartagena, Spain (e-mail: rafael.asorey@upct.es).

Luis M. Correia is with the IST/INESC-ID/INOV, University of Lisbon, 1649-004 Lisbon, Portugal (e-mail: luis.m.correia@tecnico.ulisboa.pt).

Concepcion Garcia-Pardo is with the Institute of Telecommunications and Multimedia Applications, Universitat Politècnica de Valencia, 46022 Valencia, Spain (e-mail: cgpardo@iteam.upv.es).

Krzysztof Wojcik is with the 2nd Department of Internal Medicine, Faculty of Medicine, Jagiellonian University Medical College, 31-008 Kraków, Poland (e-mail: krzysztof.wojcik@uj.edu.pl).

Kenan Turbic is with the Institute for Communication Technologies and Embedded Systems, RWTH Aachen University, 52074 Aachen, Germany (e-mail: turbic@ice.rwth-aachen.de).

Pawel Kulakowski is with the Institute of Telecommunications, AGH University of Science and Technology, 30-059 Kraków, Poland (e-mail: kulakowski@agh.edu.pl).

Digital Object Identifier 10.1109/JIOT.2022.3215884

## I. Introduction

COMMUNICATION by humans has been considered in the last decades as mobile and wireless communications, i.e., enabling users to communicate with other people, to have access to information, e.g., downloading files, and more recently to present information, e.g., usage of social media. This type of communication has been focused on using a mobile phone as a terminal, where users take action to exchange information. Nevertheless, it is clear that mobile phones will no longer be the preferred terminals of the future. Spectacles are an alternative (from the very first Google Glasses [1] to recent RayBan/Facebook ones [2], at the time of writing this article), and wearable devices in general present themselves as a trend to be explored. Moreover, in the last years, the Internet of Things (IoT) has emerged as a new perspective to communications. It has made machines communicating with each other, for the benefit of people, via a variety of terminals like sensors and actuators, and without user's intervention. 5G (the fifth generation of mobile cellular communications systems) is definitely taking a step into this direction, by enabling machine-based services that were not possible before. Massive machine type communications (MMTCs) are a clear example, as are ultra-reliable low latency communications (URLLCs).

Body area networks (BANs) have been suggested for many years, basically focusing on communications among in/on-body and wearable devices, and external networks, such as cellular ones or WiFi [3]. The list of applications for this type of networks has increased along the years, ranging from health to sports, encompassing military, police and civil protection ones, and reaching entertainment as well. There is already a wide body of knowledge in this area, although many aspects are still being researched (e.g., the impact of human mobility at several levels). Technology is already much developed in the area of wearable devices, and commercial offers already exist. Nevertheless, most of the work has been focused on the system and network aspects, not going much beyond on the issues related to communication within external or internal networks, like communication inside the human body.

Nano-networks are a more recent research topic, addressing communications inside the human body by devices that have dimensions of the scale of micro- and nano-meters, e.g., [4], [5], and [6]. In this case, technology is still at quite an early stage and much of the research work is still being done at the theoretical level, although some prototyping can

already be found [7], [8]. The common idea is to have devices inside the human body, at various levels, either implanted or mobile, e.g., in the cardiovascular or digestive systems. These devices can usually be considered either as bio-sensors, i.e., capable of sensing and collecting information about the human body, or as bio-actuators, i.e., releasing specific drugs to prevent or treat certain diseases. Of course, the information captured by bio-sensors needs to be transmitted to external networks, and bio-actuators need to be externally controlled as well. Thus, bio-sensors/actuators usually do not have a standalone approach, rather requiring communication with external networks, but this bridging has not been much addressed so far.

The applications of these networks in the medical area are many and varied. In particular, the disorders of the cardiovascular system are of high importance, as they are one of the main causes of deaths in developed countries [9], hence, their early diagnosis being very helpful to decrease the level of their fatal consequences.

Up to now, *networks* have been mentioned, but challenges do not occur only at the network level, and the system level also requires much exploration, e.g., frequencies bands, channel models, energy efficiency, and impact of human behavior, just to name a few topics. In order to have a complete view of a nano-network application, we should address as well the way that communication is established between this network and the external one. BANs present themselves as a good relay option, since nano-nodes cannot communicate directly with external networks. A number of papers have already mentioned this global perspective, e.g., [10], [11], [12], [13], and [14], but until now none has presented a global analysis from the network and system perspectives, which is the novelty of the current paper.

This article deals with the problem of an artery occlusion, which is a fatally dangerous situation when the artery is blocked by a detached thrombus, i.e., a blood clot. This article presents a new diagnostic system being able to detect artery occlusion, with suitable bio-sensors, and to prevent its consequences, with bio-actuators able to release appropriate medicines. Bio-sensors/actuators communicate with external devices via a bidirectional network composed of nano-nodes circulating in the cardiovascular system together with intrabody and body area components. This article contribution is both in the area of system design, by proposing a complete architecture of the diagnostic system, and in its validation, with the aid of a provided mathematical model.

This article is structured into nine more sections, besides the current one. Section II presents the medical applications related to the human cardiovascular system. Section III shows the global network architecture, from the nano-nodes to external networks, with interfaces and frequency aspects. Then, Section IV addresses the nano-network model, more specifically the flow of the nano-nodes together with the communication system aspects, while Section V discusses the estimation of the number of nano-nodes required to detect a problem and of the probability of activating a bio-actuator, both in an analytical perspective. System and communications aspects for the intrabody network are addressed in Section VI, and for the body area and the external networks in Section VII. Finally, an analysis of the global system performance is done in Section VIII, a discussion on technology readiness is presented in Section IX and conclusions are drawn in Section X.

## II. Medical Applications

Modern medicine relies on many diagnostic techniques for establishing patients diagnosis, monitoring diseases course, and getting therapy results. The human body is an extremely complicated machine where various phenomena occur at the mechanical, biochemical, or electrical levels, among others. As a consequence, there are plenty of methods to assess different functions of our organism, ranging from single molecules to cells and, including organs (e.g., heart or liver) and whole systems (e.g., circulation or respiratory tract).

When we analyze the process of collecting information in different diagnostic procedures, in most cases it is a one-way process, where some parameters (e.g., the concentration of certain molecules, temperature, or images) are measured and sooner or later evaluated by a physician. However, there is a large group of disorders of the circulation and respiratory systems requiring a swift diagnosis and treatment in order to avoid serious irreversible damages or even death [15], [16], [17]. The first goal of diagnostic methods in these scenarios is to get the necessary information/parameters to identify the problem as soon as possible, followed by an immediate therapeutic intervention to restore the proper functioning of the damaged system. Thus, these situations require two-way communications: 1) out of the body for reporting the medical data gathered by diagnostic systems and 2) into the body for initiating therapeutic actions by medical staff.

An area that is especially fragile and prone to numerous dangerous situations is the human cardiovascular (i.e., the bloodstream) system, responsible for about 40% of human deaths in EU Member States [9]. One of the most common disorders is an artery occlusion, which means a decrease or total blockage of blood flow. The continuous and effective performance of the circulation system is fundamental for all other organs functions, thus, an occlusion of blood vessels, especially arteries, leads to a decrease of blood supply, i.e., the oxygen and nutrients are not delivered to cells, followed by necrosis of ischemic tissues/organs. On the other hand, other disorders, such as bleeding (i.e., blood loss due to vessel damage), are also potentially critically dangerous and require immediate actions. In most cases, a suspicion of vessel occlusion is made indirectly and based on some typical symptoms or results from basic measurements, such as blood pressure or heart rate. Advanced laboratory or invasive techniques [percutaneous coronary intervention (PCI)] are applied to identify the precise location of the problem and to start therapy, such as stent implantation or fibrinolysis, required to restore blood flow [15], [16], [17].

The most relevant situations when an artery occlusion requires a prompt reaction, to prevent serious irreversible damages, include brain stroke [15], myocardial infarction, i.e., heart attack [16], and pulmonary embolism (PE), a condition when a detached thrombus is flowing with blood and may

block pulmonary arteries in some locations [17]. In all these cases, a patient needs to be admitted to a hospital and the optimal time to initiate therapy should not exceed 2 to 3 h. Occlusion of arteries in pulmonary circulation requires a treatment different from arteries in the systemic circulation, and also the treatment of a brain stroke is not the same as in the case of a myocardial infarction. Thus, immediate and precise information from inside the body about the location of an occluded artery would allow a proper planning of the therapy schedule and drug selection. In some cases, communication into the body is crucial, e.g., in a severe PE affecting the hemodynamic efficiency of circulation or in a brain stroke, and proper drugs should be administrated within minutes, or up 1 to 2-h maximum. In summary, two-way communications out of and into the body are required for early diagnosis, treatment planning, and also for starting a therapy.

In this study, we focus on pulmonary blood circulation disorders, because of the simple and well-defined structure of the pulmonary artery tree. Development of this system can expand the application to the most common vascular episodes: myocardial infarction and cerebral stroke. PE can be manifested in various scenarios, from irrelevant small artery occlusions, through the embolism with acute clinical symptoms, and finally to the life-threatening massive disorder requiring immediate actions [16], [18]. A typical reference test for the diagnosis of acute PE, considered as the most reliable one, is called computed tomographic pulmonary angiography (CTPA), where a contrast agent is injected into a pulmonary artery to identify the blocked vessels (the contrast is unable to fill occluded arteries) [19], [20]. This diagnostic procedure must be then interpreted by a radiologist. If CTPA is contraindicated or its results are inconclusive, a Ventilation Perfusion (V/Q) scan can be performed, which is based on inhaled and injected radioisotopes to visualize breathing (ventilation) and circulation (perfusion) processes in all areas of the lungs [21]. Historically, it was pulmonary angiography (PA) that was the gold standard for PE diagnosis (the contrast material is injected via a catheter introduced into the right part of the heart), however, nowadays PA is considered to be inferior to CTPA [22]. Finally, also magnetic resonance angiography (MRA) was a promising diagnostic technique, but the results of large-scale studies do not recommend MRA as a first-line test due to its low sensitivity, low availability in most emergency settings and high percentage of inconclusive scans [23].

In practice, the average time between symptom onset and PE diagnosis varies between 5 and 9 days [24], [25], [26]. Even after taking such a person to a hospital, the median time from admission to examination is about 3.5 h [27] with main factors responsible for diagnosis delay being patients age, comorbidities, and PE severity. A diagnosis time prolonged over 12 h leads to increased mortality [27].

Considering all these aforementioned factors, in this article we propose a different approach where a person can be continuously monitored when she/he is leading a normal and active life. Our proposal is based on bio-sensors and bio-actuators installed in the pulmonary arteries and nano-nodes circulating in the bloodstream, Fig. 1. Monitoring by bio-sensors can

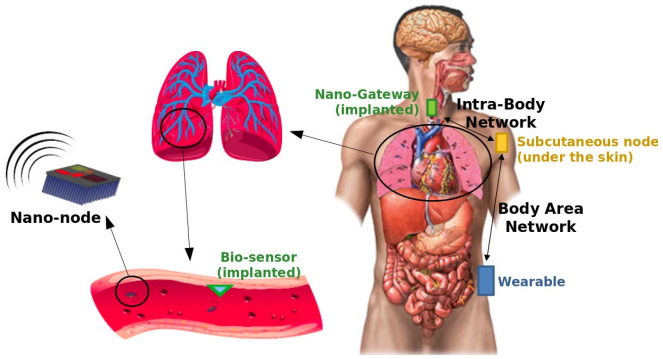


Fig. 1. Overview of the system architecture for PE prevention.

reveal the narrowing of the artery lumen before clinical symptoms appear. On the other hand, bio-actuators can release drugs locally in the region where the occlusion occurs, thus, allowing to avoid certain organs/tissues damage. Communication with an external network (and medical staff) is realized via the mobile nano-nodes and a BAN; the whole concept of a global network architecture is introduced in Section III.

It is worthwhile to stress that biotechnological capabilities, required for mounting bio-sensors/actuators into pulmonary arteries, already exist. Nowadays, the technology of intravenous interventions is well developed: there are various methods for the treatment of both arterial and vein issues, i.e., diagnostic angiography, angioplasty, atherectomy, and stenting for arterial disease [15], [28], renovascular and mesenteric revascularizations for the former, and inferior vena cava filtration, deep venous thrombosis treatment, pulmonary emboli [16], varicoceles and varicose veins, venous occlusions (chronic and acute), and arteriovenous malformations for the latter. Thus, although the implantation of bio-devices in blood vessels can be easily achieved, an open issue is still the provision of reliable two-way communications between the numerous bio-devices and the medical staff, required for the effective monitoring of blood flow, the ability for timely diagnose artery occlusion and the start of treatment before any serious damages occur.

## III. Network Architecture

The proposed system is designed to perform three functions: 1) transmitting information about a possible PE; 2) if appropriate, releasing medicines to dissolve thrombus; and 3) providing two-way communications between in-body devices and medical staff, i.e., out of the patient's body and into it. The first two functions are realized with bio-sensors (transmitting signals) and bio-actuators (releasing medicine) located in pulmonary arteries. Two-way communications require a bidirectional system transporting the information from the cardiovascular system out of the body and vice versa. It would be tempting to realize these communications directly between the bio-devices and a node located just under or on the skin, without any nano-network, but, however, this is not feasible in practice for medical reasons: equipping all bio-devices with high-range GHz interfaces would enlarge these devices to the

TABLE I
NANO AND BODY AREA DEVICES COMPOSING THE ARCHITECTURE OF THE PROPOSED SYSTEM

| | position | approximate dimensions | power supply | main functionalities |
|---|---|---|---|---|
| **bio-sensors** | static, on stents in pulmonary arteries | $5 \times 1 \times 1$ mm$^3$ | lithium/iodine battery | transmitting ID signals |
| **bio-actuators** | static, on stents in pulmonary arteries | $5 \times 2 \times 2$ mm$^3$ | lithium/iodine battery | releasing medications |
| **nano-nodes** | mobile, circulating in the vascular system | $8 \times 8 \times 3$ µm$^3$ | piezoelectric generators | carrying data frames |
| **nano-gateway** | static, on the wall of superior vena cava | $20 \times 3.5 \times 2$ mm$^3$ | lithium/iodine battery | intermediary node |
| **subcutaneous node** | static, under the skin on the chest | $20 \times 20 \times 3$ mm$^3$ | lithium/iodine battery | intermediary node |

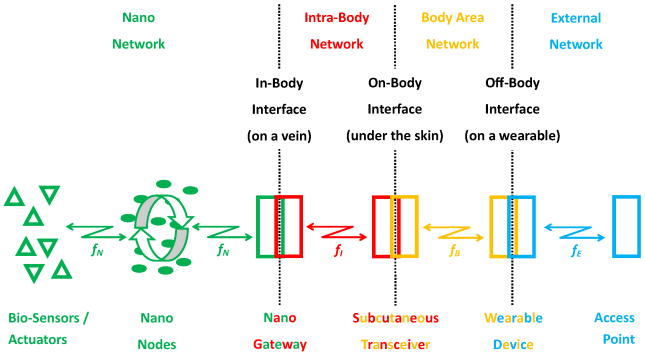


Fig. 2. Network architecture providing full communications between nano-devices and the external network.

size of centimeters, rendering them useless, having in mind the diameter of pulmonary arteries.

Fig. 2 shows a global view of the whole proposed system, with various subnetworks and corresponding interfaces. Additionally, Table I summarizes essential parameters of system components. In what follows, we describe these components in detail.

1) *Bio-sensors* are medical devices located in specific inner parts of the body, i.e., organs or tissues, measuring certain parameters. In the considered system, we assume that there are static bio-sensors mounted in pulmonary arteries for detecting a possible embolism. Pulmonary arteries are part of the vascular system, which is very well known (e.g., [29]); it has one main artery divided into three smaller ones (2nd level), which in total then divides into eight branches (3rd level), then into 20 branches (4th level), and so on, until the 17th level having about $3 \times 10^8$ branches. For the considered application, we suggest to have bio-sensors down to the 4th level of the pulmonary system, at each of the 20 arteries, since this level is a tradeoff for the location of bio-sensors: on the one hand, the blockage of the higher level arteries (1st, 2nd, and 3rd) can be detected at the 4th level, and we just observe more than one 4th level arteries blocked; on the other hand, lower level (>4th) arteries are too thin to cause severe hemodynamic problems, so investigating all these single small arteries is not effective. Bio-sensors are simple devices, just transmitting their ID as beacons in the THz band. We assume that the bio-sensor implantation procedure is based on a well-known stent technique [30], however, the stent is used here not for artery stenosis, but for creating a stable structure to mount a bio-sensor. Each stent is a tiny plastic tube (if needed, can be bioresorbable) inserted into the lumen of a blood vessel, with around 5-mm length and strut thickness of 50$\mu$m [31]. The bio-sensor is mounted on the stent just by the artery wall. It is important to note that a bio-sensor located in the artery cannot measure the thrombus directly, as it can occur at any place of the artery. Instead, we propose that each bio-sensor is immobile and constantly transmits a frame with its ID number, which can be received by nano-nodes flowing in the blood. When the blood flow is stopped by a thrombus in a specific artery, nano-nodes cannot flow there and none of them collects a frame with the respective ID. Consequently, after a certain period of time, biased statistics can be observed among all frames collected in the system: the numbers of frames collected from bio-sensors will increase for all of the bio-sensors except of this one in the blocked artery. This is investigated in detail in Section VIII.
2) *Bio-actuators* are medical devices of another type: upon receiving a request, they are able of performing an action, e.g., to release medication such as alteplase, which causes the thrombus to dissolve [32], [33]. We assume that bio-actuators are placed at the first three levels of the pulmonary system at each of the 1+3+8 arteries, so, after a thrombus is detected by a bio-sensor, the alteplase can be released from a higher-level artery. The predicted dimensions of bio-actuators are slightly larger than bio-sensors ones, as they keep alteplase inside (see Table I), but the respective arteries (first three levels) are also wider.
3) *Nano-nodes* are relay nodes passing information from bio-sensors/actuators to the nano-gateway or vice-versa. Nano-nodes are circulating with the blood in the cardiovascular system [34] in a so-called flow-guided nano-network [35]. They are of the size of about 8 µm and, because of their antenna size, they can communicate only in the THz band where range is limited to 1 to 2 mm [36], so they cannot communicate further than in the cardiovascular system. These nodes have very restricted processing capabilities and a limited battery that can be periodically charged with a piezoelectric generator, thus, they can only transmit/receive at a certain time and only if the battery is loaded enough.
4) A *nano-gateway* performs the function of a mediator between nano-nodes and the intrabody network. In the considered system, we propose to locate it on the wall of the superior vena cava, which is a large vein (a diameter about 2 cm) in the human chest [37], well accessible

for medical surgery operations and only 4-cm under the skin. The nano-gateway has two wireless interfaces: a THz one to communicate with the nano-nodes and a GHz one with a larger range allowing for communication with the subcutaneous transceiver. A direct wireless link between the nano-gateway and a wearable is not feasible, because of the high attenuation of body tissues.

5) A *subcutaneous transceiver* located just under the skin mediates between the intrabody and BANs, enabling communications between the aforementioned nano-gateway and a wearable device. A single wireless interface is sufficient here, as both links, to the nano-gateway and to the wearable device, can be realized at the GHz band. This latter link, between the subcutaneous transceiver and the wearable device, should use a standard communications system (e.g., Bluetooth or WiFi), so that a wide range of devices can be used, thus, providing a wide range of options for these devices.
6) A *wearable device*, e.g., a smartwatch, a smartphone, a smart bracelet, or another device enabling a connection to an external network. It also acts as a relay node, between the subcutaneous transceiver and the external network, with two wireless interfaces, the latter being most probably based on WiFi or a cellular system. As this type of device is from a common commercial technology, its description is considered to be out of the scope of this article.

The whole network operates in the following manner. Bio-sensors constantly transmit frames containing their ID, which are collected by mobile nano-nodes and later passed onto the nano-gateway. Frames are aggregated at the nano-gateway and transmitted to the subcutaneous transceiver, which forwards them to the wearable device, which in turn sends them to the external network. Medical staff can analyze the number of frames from all bio-sensors and check if their statistics are biased, i.e., if there are bio-sensors that do not deliver their frames, which can imply the blockage of the respective artery. Then, if the medical staff decides so, a request is sent to a specific bio-actuator to release a medicine dissolving the thrombus and unblocking the artery. The request is sent via a reverse link: via the wearable device, the subcutaneous transceiver, down to the nano-gateway, which broadcasts it to the nano-nodes. These nodes transmit it and eventually the frame is passed onto the proper bio-actuator.

This overall system is a complex mixture of technologies, at quite different stages of development. Basically, while higher frequencies and smaller scale nodes (i.e., THz bands and nano-networks) are still at an early research stage, the opposite lower frequencies and larger scale nodes (GHz frequencies for the intrabody and BANs) are already offered commercially. Therefore, naturally, in what follows, attention is mostly paid to nano-networks, and then addressing the other subnetworks with a decreasing focus.

## IV. Flow-Guided Nano-Network Model

The flow-guided nano-network model is derived from [35]. Nano-nodes circulate in the blood flow of the circulatory system, transmitting data to the nano-gateway that, in turn, sends data to the upper layers of the global network, up to the external network. The nano-device architecture used in this work is derived from [34], where a realistic nano-node model based on current technologies is presented. In this sense, the power and computational limitations of the nano-nodes translate into the following: 1) they can only transmit one data frame per battery charging cycle and 2) they do not know the position of the gateway. The model has been extended and generalized to support our optimization problem.

### A. Assumptions

The following assumptions are made (a summary of all variables used in this article is given in Annex.)

1) There are $N$ nano-nodes uniformly distributed along the flow, being in a closed circuit, i.e., continuously flowing in the vascular system. The total volume of the circuit is $V_{\text{net}}$.
2) A nano-node requires, on average, a time $\overline{T_{\text{cir}}}$ to complete a round.
3) The battery of a nano-node is charged at time intervals $T_{\text{cha}}(t)$ by means of piezoelectric nano-tubes as described in [34]

$$T_{\text{cha}}(t) = \frac{1}{f_{\text{cha}}(t)} \tag{1}$$

where $f_{\text{cha}}(t)$ indicates that the recharging frequency can vary over time. Due to energy constraints, as described in [35], a nano-node only transmits one data frame per battery charging cycle to maximize coverage. Moreover, $f_{\text{cha}}(t)$ is bounded

$$f_{\min} \leq f_{\text{cha}}(t) \leq f_{\max} \tag{2}$$

and the average charging frequency is $\overline{f_{\text{cha}}}$, e.g., the heart rate.
4) Without loss of generality, let us assume that there are regions in the flow in which a nano-node is within the coverage zone of a nano-gateway, a bio-sensor or a bio-actuator of volume $V_{cv}$. A nano-node moves at an average speed $v$ in the coverage zone, and since a nano-node cannot receive/transmit more than one frame when crossing this volume, the probability of a nano-node being in a coverage zone, $p_{cv}$, is modeled as follows:

$$p_{cv} = \frac{V_{cv}}{V_{\text{net}}}. \tag{3}$$

5) A nano-node does not know if it is within a coverage area, therefore, any nano-node attempts to transmit/receive a data frame during every battery charging cycle, which has two main consequences.
   a) Half of the energy is used in the transmitting mode and the other half in the receiving one.
   b) In order to minimize collisions, after battery charging all nano-nodes first listen to the channel for frame transmissions, nano-gateways, or bio-sensors transmitting at this moment. Once channel listening is over, all nano-nodes attempt to transmit a frame, therefore, this avoids frame collisions between

transmissions of bio-sensors and nano-nodes as they will transmit in different slots.

6) A successful frame reception by a nano-node from a nano-gateway or a bio-sensor takes place if it starts and ends within its coverage volume. We define this region as the reception zone, with a volume $V_{rx}$, $V_{rx} < V_{cv}$, thus, the probability of a nano-node being in the reception zone is

$$p_{rx} = \frac{V_{rx}}{V_{\text{net}}} < p_{cv}. \tag{4}$$

7) A successful frame transmission from a nano-node to a nano-gateway or a bio-actuator takes place if it starts and ends within the coverage volume and no frame collision occurs. We define this region as the transmission zone, with a volume $V_{tx}$, $V_{tx} < V_{cv}$, thus, the probability of a nano-node being in the transmission zone is

$$p_{tx} = \frac{V_{tx}}{V_{\text{net}}} < p_{cv}. \tag{5}$$

8) A frame collision occurs if one or more transmissions start or end within the nano-gateway or bio-actuator coverage zone while another transmission in the transmission zone is taking place. Note that a node located outside the coverage zone can cause a collision if its transmission ends within this volume. We define the region in which a node may cause collisions as the collision zone of volume $V_{cx}$, $V_{cx} > V_{cv}$, thus, the probability of a nano-node being in the collision zone is

$$p_{cx} = \frac{V_{cx}}{V_{\text{net}}} > p_{cv}. \tag{6}$$

9) We consider frames consisting of three fields: a) *addressing* of length $\lambda_h$ bytes; b) other fields of length $\lambda_o$; and c) *data payload* of length $\lambda_d$. Thus, the frame size is

$$\lambda_f = \lambda_h + \lambda_o + \lambda_d. \tag{7}$$

10) The frame duration, $t_f$, depends on the frame size, $\lambda_f$ and on the transmission bit rate, $R$; taking $t_f$ as the time required to transmit a frame

$$t_f = 8\lambda_f / R \tag{8}$$

then $t_f \leq T_{\text{cha}}(t)$.

### B. Channel Model

The channel model is based on the one described in [38]. Basically, the required transmission power for a frame, $P_{tx}$, depends on the gateway receiver sensitivity $P_{rx\ \text{min}}$, path loss coefficient $\alpha_{\text{lin}}$, and distance $d_{mm}$

$$P_{tx\ [\text{dBm}]} \geq P_{rx\ \text{min}\ [\text{dBm}]} + \alpha_{lin\ [\text{dB/m}]}\, d_{mm\ [\text{m}]} \tag{9}$$

where $P_{rx\ \text{min}}$ and $\alpha_{\text{lin}}$ are assumed to be constant, whereas $d_{mm}$ can be configured according to the energy available in a nano-node battery.

Regarding the modulation to transmit data, we assume the well-accepted model for the transmission of femto-pulses, along with an on–off keying modulation [39]. This modulation assumes that energy is only consumed when transmitting bits with a logic value equal to 1, 0 being transmitted as silence, therefore, no energy is consumed in the transmission of the latter. The radio channel corresponds to a sequence of time windows during which a bit is transmitted using an electromagnetic pulse of a duration of $t_p = 100\,\text{fs}$. The duration between two consecutive bits is, in general, much longer than $t_p$.

For the sake of simplicity, we assume that the energy required to transmit or to receive a bit is similar to the one for a bit 1 symbol, $E_{b=1}$, being expressed as follows:

$$E_{b=1} = P_{tx}\, t_p \tag{10}$$

whereas to transmit a bit 0 symbol, we have $E_{b=0} = 0$.

From (10), it is straightforward to derive that the maximum required energy to transmit/receive a frame, $E_{f\ \text{max}}$, corresponds to the case in which all bits in a frame of size $\lambda_f$ are the bit 1 symbol. Moreover, if the amount of energy that a nano-node can store when it is fully charged is denoted as $Q$, and a nano-node can receive/transmit a frame at every cycle, the following must hold:

$$E_{f\ \text{max}} = 8\,\lambda_f\, E_{b=1} \leq \frac{Q}{2}. \tag{11}$$

The inequality in (11) shows that higher values of $\lambda_f$ lead to lower values of $E_{b=1}$ and, consequently, to lower transmission powers and a smaller coverage area [following (9)].

Although it is out of the scope of this article, we can assume that when a nano-node does not transmit, it acquires data or performs other tasks. In other words, a nano-node keeps consuming energy even if it is not transmitting. This power consumption is disregarded in our model, but it can be approximated by a fixed quantity of energy that can be added to $Q$.

### C. Coverage Zone Model

In this article, we follow a simple and intuitive model for the coverage zone, the main assumptions being summarized as follows.

1) There is a spherical volume of radius $d_{mm}$ [see (9)] around the gateway in which a transmission/reception can be successful if no frame collision occurs. All transmissions/receptions outside this region will fail. Frame collisions can happen when nano-nodes are transmitting to a nano-gateway or a bio-actuator, but not if it is the nano-gateway or the bio-sensor that is transmitting and nano-nodes are only listening.
2) The antennas of the nano-gateway, bio-sensors, bio-actuators, and nano-devices are isotropic.
3) The coverage zone, $V_{cv}$, is defined by the intersection of a sphere of radius $d_{mm}$ centered at the nano-gateway, the bio-sensor/actuator and a cylinder with a diameter equal to the respective vein or artery, $D_{cyl}$. All these distances are in the order of 1 mm at most. The full derivation how to calculate this intersection for the known values of $d_{mm}$ and $D_{cyl}$ can be found in [40].

It is also necessary to consider the mobility of nodes in such flow-guided nano-networks. To this end, it can be considered

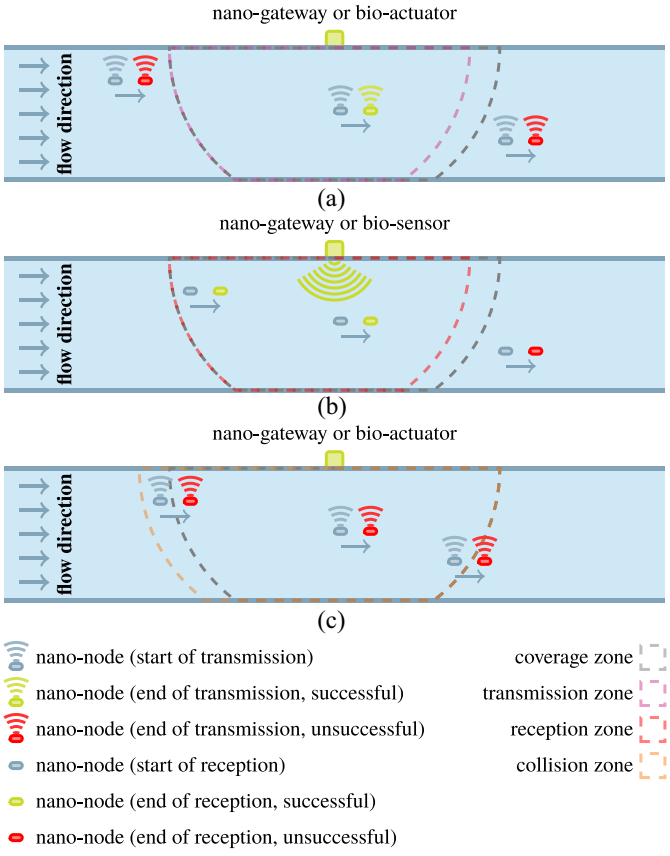


Fig. 3. Illustration of successful transmissions and receptions, and of collisions. (a) Successful transmission. (b) Successful receptions. (c) Collisions.

that a nano-node moves at an average speed $\bar{v}$ (it depends on the position of the nano-gateway or of the bio-sensor/actuator) in the flow and that frame transmissions last $t_f$, the distance traveled by the nano-node, $d_{nn}$, being

$$d_{nn} = \bar{v}\, t_f. \tag{12}$$

This derivation entails two new assumptions.

1) In order to successfully transmit/receive a frame, a transmission must start and end within the coverage volume, thus, if the node is close to leaving the coverage volume when the transmission/reception starts, then there is no time to finish it within this zone and the transmission fails. For this reason, an additional value of the successful transmission/reception zone, $V_{tx} = V_{rx}$, should be defined, which is smaller than the coverage zone, $V_{cv}$.
2) A collision occurs when two or more nano-nodes transmit within the coverage zone, thus, it is necessary to consider transmissions starting outside the coverage zone but ending inside it. For this reason, the volume corresponding to the collision zone, $V_{cx}$, must be also considered.

The values of $V_{tx} = V_{rx}$ and $V_{cx}$ can be calculated in a way similar to $V_{cv}$, having $d_{mm}$, $D_{cyl}$, $\bar{v}$, and $t_f$, by using the derivation from [40]. Fig. 3 illustrates the differences among coverage, transmission, and collision zones for different scenarios.

To summarize, nano-node movement reduces the volume of the transmission zone, increasing the corresponding volume of the collision zone. Consequently, as it is not possible to set up the flow speed, a shorter $t_f$ value (and shorter frame size, $\lambda_f$) improves the probability of successful transmissions. Moreover, in our model, the following condition must hold:

$$d_{nn} < 2\, d_{mm}. \tag{13}$$

This condition guarantees that any arbitrary node crossing near the nano-gateway or the bio-actuator will have the chance to successfully transmit/receive a frame. Note that, for negligible values of $d_{nn}$, there are no transmission range requirements, although higher values of $d_{mm}$ lead to higher coverage, transmission/reception, and collision volumes. For nonnegligible values of $d_{nn}$, inequality (13) guarantees that volume $V_{tx} = V_{rx}$ is large enough to allow complete frame transmissions ($V_{tx} = V_{rx} > 0$).

An example of transmissions/receptions and collisions can be found in Fig. 3. For a successful transmission, a nano-node must be alone within the transmission zone when it starts sending a frame; note that only one successful transmission is possible at the same time. Similarly, a successful reception happens if a nano-node is within the reception zone when the transmission starts; in this case, more than one successful reception is possible in the reception zone as no collisions can happen. Collisions can happen if two or more nano-nodes start or end a transmission within the coverage zone.

### D. Frame Structure and Duration

There are some proposals in the literature dealing with MAC protocols for nano-networks [41], [42], [43], but none consider the particularities of flow-guided nano-networks. It is outside the scope of this article to provide a detailed frame structure (which depends on the particular protocol implementation), however, it is important to differentiate between the size of the frame data payload and the remaining fields, thus, we propose a very simple frame structure that is used in our optimization problem.

1) *Addressing Field of Size $\lambda_h$:* We assume that a frame contains at least two addresses (for sender and receiver, respectively), hence, if the nano-network contains $N$ nano-nodes plus a gateway, then the following must hold:
$$\lambda_h \geq 2\left\lceil \frac{\log_2(N+1)}{8} \right\rceil. \tag{14}$$
Although the receiver address field could be removed if a broadcast transmission model would be assumed, not doing so allows transmitting to specific nodes or groups of nodes. In any case, removing it or not has a negligible impact on the frame size and system performance.
2) *Other Fields of Constant Size $\lambda_o$:* Within this category checksums, frame size, etc., can be included.
3) *Data Payload of Size $\lambda_d$:* Its size is determined by medical application requirements.

From this basic frame structure, we derive the total frame size, (7). Regarding the time required to transmit a frame, $t_f$, when the nano-node transmits at a bitrate $R$, it is defined

by (8). Moreover, $t_f$ is subject to the constraint $V_{tx} = V_{rx} > 0$, i.e., as longer values of $t_f$ reduce $V_{tx} = V_{rx}$, there is a limit for $t_f$, otherwise, no transmissions are possible.

### E. Nano-Node Transmission Model

The throughput of a flow-guided nano-network, $\theta$, has already been presented in [35] in frame/s, being reformulated in bit/s as follows:

$$\theta = \frac{8\,\lambda_d\,N\,\overline{f_{\text{cha}}}\,V_{tx}}{V_{\text{net}}}\left(1-\frac{V_{cx}}{V_{\text{net}}}\right)^{N-1}. \tag{15}$$

Expression (15) represents the amount of data that can reach the nano-gateway, being related to the probability of a nano-node performing a complete transmission within the coverage volume when no collision occurs. As proved in [35], the throughput increases as the number of nano-nodes grows to a certain value, beyond which increasing the number of nano-nodes causes the throughput to decrease, since the probability of collisions starts to be significant (there are too many nano-nodes in the flow-guided nano-network).

Additionally, the work in [35] shows interesting facts about these flow-guided nano-networks.

1) There is a value of the number of nano-nodes, $N_\theta$, that maximizes throughput for any network setup, which is derived from (15)
$$N_\theta \approx \frac{V_{\text{net}}}{V_{cx}}. \tag{16}$$
2) The size of the coverage volume is not relevant to achieve a larger throughput, however, following (16), a higher value of $V_{tx}$ and $V_{cx}$ requires fewer nano-nodes to achieve maximum throughput.

Note that the time required for a nano-node to complete a round in the flow-guided nano-network, $T_{\text{cir}}$, is not significant in terms of throughput, the relevant parameters being $V_{\text{net}}$, $V_{tx}$, $V_{cx}$, and $N$ ($V_{tx}$ and $V_{cx}$ can be generally approximated by $V_{cv}$ for negligible values of $d_{nn}$).

## V. Estimation of Implementation Parameters

The goal of the following analytical estimation is to obtain a minimum threshold of the number of nano-nodes that guarantees with a given probability ($p_{Qd}$) that no false detection is performed. To this end, we can start by calculating the average number of successful frames received by the nano-nodes during a round

$$\overline{r_T} = N\overline{f_{\text{cha}}}\,\overline{T_{\text{cir}}}\left(\frac{V_{rx}}{V_{\text{net}}}\right) \tag{17}$$

thus, as a Uniform Distribution is assumed for nano-nodes and a nano-node cannot receive more than one frame per round, the probability that a nano-node receives a frame is

$$p_{rx,T} = \frac{\overline{r_T}}{N} = \frac{\overline{f_{\text{cha}}}\,\overline{T_{\text{cir}}}\,V_{rx}}{V_{\text{net}}}. \tag{18}$$

After $\tau$ time slots, the probability of a nano-node having received at least a frame from a bio-sensor can be modeled as follows:

$$p_{rx,T,\tau} = 1-\left(1-p_{rx,T}\right)^{\tau/\left(\overline{f_{\text{cha}}}\,\overline{T_{\text{cir}}}\right)}. \tag{19}$$

The system fails if the artery in which the bio-sensor is placed is not blocked and no frame transmitted from it arrives to the gateway, thus, for every time slot, a failure happens if the gateway receives a frame not containing any information from the bio-sensor or does not receive anything, equivalently, being the probability of not receiving a successful notification from the bio-sensor, $p_f$, which can modeled by

$$p_f = 1-\frac{N\,V_{tx}}{V_{\text{net}}}\left(1-\frac{V_{cx}}{V_{\text{net}}}\right)^{N-1}p_{rx,T,\tau}. \tag{20}$$

The probability that after $\tau$ time slots no bio-sensor detection happens is

$$p_{f,\tau} = (p_f)^\tau. \tag{21}$$

As the final goal is to dimension the network to obtain a $p_{f,\tau}$ bellow a given threshold, i.e., $1-p_{Qd}$, the following must hold:

$$p_{f,\tau} \le 1-p_{Qd}. \tag{22}$$

If $1-p_{Qd} \to 0$, (22) can be approximated by

$$\frac{\tau\,N\,V_{tx}}{V_{\text{net}}}\left(1-\frac{V_{cx}}{V_{\text{net}}}\right)^{N-1}p_{rx,T,\tau} \ge p_{Qd}. \tag{23}$$

Beyond the detection of a blocked artery, it is also important to estimate the probability of receiving a frame if the artery is nonblocked. In this sense, $\tau$ can be interpreted as the time in which the nano-node remembers it has received a message from a bio-sensor. In other words, a nano-node remembers a frame reception from a bio-sensor during $\tau$ time slots. Thus, let us define $\epsilon$ as the elapsed time slots since the last bio-sensor detection, and $p_{d,\tau,\epsilon}$ as the probability of receiving a frame before $\epsilon$ time units if a nano-node remembers a bio-sensor frame reception for $\tau$ time units. From (21) it is straightforward to derive $p_{d,\tau,\epsilon}$ as follows:

$$p_{d,\tau,\epsilon} = 1-(p_f)^\epsilon. \tag{24}$$

Expression (24) converges to 1 as $\epsilon$ increases, this convergence being faster for higher values of $\tau$. This is consistent with the fact that higher values of $\tau$ increase the probability of more nano-nodes in the system with received frames from the targeted bio-sensor.

Finally, it remains to obtain the estimation of the probability for activating a bio-actuator. Once a bio-actuator has to be activated as a consequence of a medical issue, it is important that this activation can happen within a given deadline with a high probability. To this end, we assume that nano-nodes receive the order of activating a given bio-actuator from the nano-gateway, and that, at the beginning, no nano-node has received an activation order.

Thus, similarly to (19), the probability that a nano-node receives an activation order in $M$ rounds can be obtained as follows:

$$p_{rx,T,M} = 1-\left(1-p_{rx,T}\right)^M \tag{25}$$

from which it is possible to calculate the probability of successfully performing an activation of a bio-actuator in round

$M$, $p_{a,M}$, as follows:

$$p_{a,M} = 1 - \left(1 - \frac{N\,V_{tx}}{V_{\text{net}}}\left(1 - \frac{V_{cx}}{V_{\text{net}}}\right)^{N-1} p_{rx,T,M}\right)^{\overline{f_{\text{cha}}}\,\overline{T_{\text{cir}}}}. \quad (26)$$

The final goal is to dimension the network so that a bio-actuator gets activated in less than $\phi$ rounds with a very high probability, $p_{Qa}$

$$\prod_{k=1}^{\phi}\left(1 - p_{a,k}\right) \leq 1 - p_{Qa}. \quad (27)$$

Having established the model for the nano-network, the other subnetworks need to be characterized as well.

## VI. Intrabody Network

Once the information carried by nano-nodes is collected by the nano-gateway, its delivery toward a device outside of the body is another important challenge. As aforementioned, we propose an intrabody link between the nano-gateway and a subcutaneous implant using radio frequency techniques in order to overcome the gap between the circulatory system at the nano level and the outer level of the body, this approach being illustrated in the right part of Fig. 1.

Intrabody (also called in-body or implanted) radio communications have been widely addressed in the literature. Until today, the medical implant communications service (MICS) band at [402, 405] MHz has been used by medical devices for data transmission, due to the low losses of body tissues at these frequencies. However, its offered low data rates and especially the antennas large size at these frequencies lead to the exploration of higher frequency bands [44], [45].

Recently, the ultra-wideband (UWB) technology has been proposed for the operation of ingestible devices due to its large bandwidth, [3.1, 10.6] GHz, high data rates, low power consumption, and miniaturization capabilities [46]. However, human body tissues exhibit a large attenuation at UWB frequencies and this attenuation is frequency dependent. Thus, the lower part of the UWB band [3.1, 5.1] GHz has been recommended for wideband in-body communications [47], [48], especially for a wireless capsule endoscopy (WCE) scenario where high-quality video transmission is required.

The industrial, scientific, and medical (ISM) band, [2.4, 2.5] GHz, has been also proposed for the operation of in-body devices. Despite the lower offered data rates compared to UWB, it can provide a good tradeoff among miniaturization capability, path loss, and occupied bandwidth, thus, being an ideal technology to transmit data from inside the human body in case of moderate data rates. More specifically, the ISM band has been recently proposed to be used in the future generation of leadless pacemakers, where an in-body antenna will be implanted inside the heart and a subcutaneous antenna is configured as a receiver. It was found that the ISM band is optimal for this kind of communications, due to the combination of the inherent path loss of the biological tissues at these frequencies and the high achievable efficiency of the antenna [45].

In the last years, several works have analyzed communications in this area, using the 2.4-GHz band for cardiac applications. Concretely, Bose et al. [45] analyzed implant-to-subcutaneous communications, for three different positions of the subcutaneous receiver. It was found that the path loss (also called coupling in other studies) was optimal (minimum) when installed subcutaneously in the outer wall of the abdomen. Nevertheless, this position can cause discomfort to the patient in a real application, which the authors propose to solve with a multinodal solution. In contrast, location on the shoulder could be the best for the patient, with the drawback of increasing the path loss nearly 10 dB.

Antennas also play a key role in link evaluation. Antennas performance not only depends on their own design, but also of the surrounding tissues where they operate [49]. This is particularly important for implanted antennas at GHz frequencies, where surrounding organs commonly are high-water content tissues with large permittivity, thus, being extremely important to design and optimize antennas considering all tissue layers present between the implanted transmitter and the subcutaneous receiver [50].

Several candidates for both implanted and subcutaneous antennas that have been proposed in the literature for the cardiac scenario so far. In [45], [51], and [52], implanted and subcutaneous antennas have been proposed. However, all the designs are not flexible enough for a real application over the surface of the vena cava. Faisal et al. [53] presented a flexible antenna to operate in the scalp, which is a much less delicate area compared to the superior vena cava. A similar situation was found in [54], where the proposed ISM antenna is neither flexible nor designed to operate deeply implanted. As mentioned before, the final performance of the in-body link has to be taken into account, which is influenced by the definite antenna design.

Considering the scenario of this work, where the gateway is attached to the superior vena cava, the arrangement of both in-body and subcutaneous antennas is very similar to the one proposed in the literature for leadless pacemakers. In this scenario, the signal needs to be transmitted from the external wall of the superior vena cava (with a depth of 4 cm) to a remote receiver, which implies data transmission throughout the thorax; besides, the antenna's surrounding tissues are nearly the same as in the cardiac scenario (blood, veins, muscle, and subcutaneous fat). Therefore, we can conclude that the ISM 2.4 GHz is the most suitable band to transmit data gathered from the nano-network to the superior vena cava, due to the affordable path losses at these frequencies along with their offered moderate data rates. It should be noted that the implanted and subcutaneous antenna models already outlined for cardiac applications can be used as a starting point for the design of antennas for the intrabody link. The main difference here is that the in-body antenna should be really ultra flexible and tiny, in order to be implanted inside the human body, and particularly over the surface of the vena cava. Current research on biocompatible and flexible materials shows promising achievements in the near future in this field [55], [56], [57]. Similar requirements are needed for the subcutaneous implant, although

its features are not so restrictive in terms of flexibility and size.

## VII. Body Area and External Networks

Having delivered the sensory information from the nanonetwork to the subcutaneous node, the remaining task is to further transport data to a nearby wearable device or communication infrastructure, Fig. 1. Still, in order to do so, given that the subcutaneous transceiver is a very low-power device, the approach taken is that this transceiver establishes an on-body communication to a wearable device (e.g., a smartphone or a smartwatch), and then this device enables the off-body communication to the external network (via a cellular system or WiFi). Nevertheless, a discussion on this matter is in order.

With the transceiver placed under the skin, to minimize tissue penetration losses, communication to the external network can be realized in two ways. In one approach, we can assume that the transceiver is capable enough to establish a connection directly to the external network, but this seems a reasonable choice only if this link is established over short distances, such as in specific indoor environments, e.g., hospital rooms. In another approach, we can seek for a wider range of applications, where the constraints on the small size, low-energy, and comfort typically limit the complexity of these transceivers; in this case, the link should use a wearable device as a relay, which allows for a longer off-body communication range and access to several communication technologies typically available in such devices, however, at the expense of an additional on-body communication link introduced to the data delivery chain.

On-body communications from subcutaneous devices has already gained the attention of researchers and the literature has a number of works in this area. The key problem, from the communications system viewpoint, is to characterize the channel, namely, path loss, so that one can estimate a proper link budget for the link. There are a wide number of works addressing the analysis of the path loss when one node is located subcutaneously, considering different frequencies. In [58], 403 and 923 MHz are considered with path losses lower than 15 dB for the highest frequencies and separation of 15 cm. In [59], for 1.85-GHz path losses are considerably higher because of the increment of frequency, rising up to 59 dB for a separation of 40 cm. Blauert and Kiourti [60] and Green et al. [61] addressed a subcutaneous link for the 1.4-GHz Wireless Medical Telemetry Service and 2.4-GHz ISM bands showing path loss values from 8 to 90 dB depending on the implantation depth. Besides, path loss depends on the location of the subcutaneous transceiver as well as on the one for the wearable device, being smaller when transceiver is located in the chest and a wearable device on the belt, compared when the device is a smartphone or a smartwatch.

With a number of mature radio communication technologies being available for employment in this link, most notably Bluetooth, Bluetooth Low Energy, ZigBee, and UWB being among the technologies acknowledged by IEEE 802.15.6 [62], we can expect that this link will tend not to use a brand new technology, but rather a version of these ones, with the proper modifications (e.g., to account for power limitations and to minimize interference). Moreover, in order to simplify the design of the subcutaneous transceiver, and to accommodate the low size and low power requirements, we envisage that the same system is used for the links with both the nanogateway and the wearable device, in a time-shared mode [i.e., time division duplexing (TDD)]; since the required data rates are not that high, the TDD mode can be easily implemented in the transceiver.

In both on- and off-body communication links, body-shadowing, and depolarization losses [63] play important roles, together with the impact of user dynamics, yielding a nonstationary channel [64]. Body-shadowing occurs when the user (in on- and off-body links) or another person (in off-body links) obstructs the Line-of-Sight (LoS) propagation path, thereby introducing excess losses up to 30 dB [65], [66]. The low elevation and proximity of wearable antennas to the body make this effect particularly challenging in BAN communications, where a simple user rotation brings the antenna deep into the shadowed region [67]. The main difference in body shadowing characteristics among on-body antenna locations essentially comes from the different motion dynamics.

The severity of body shadowing also varies among different scenarios. For example, losses are expected to be lower with the user walking around a room, compared to the case when the user is lying on a bed. While the diversity stemming from the existence of several propagation paths in different directions dampens the impact of individual path shadowing on the total receiver power in the former case, in the latter one the wearable antenna can find itself completely covered between the user and the bed.

Signal depolarization [68], is caused by the polarization mismatch losses due to depolarization in the propagation environment [69], [70], antenna depolarization in the proximity of the lossy body tissue [71], and to the wearable antenna rotation during motion [64]. The polarization of wearable patch antennas is reported to change from a linear one in free space to an elliptical one when placed near the body, with a shorter distance from the body yielding a higher degree of depolarization.

The dynamic rotation of antennas on arms and legs during motion results in high and variable polarization mismatch losses, compared to the nearly static antenna placements on the torso or the head. For a simple simulated scenario with the user running in [68], these losses are below 1.5 dB for the antenna on the torso, while reaching $-42$ and $-34$ dB for wrist and lower leg placements, respectively. To mitigate these effects, polarization diversity with co-located cross-polarized antennas offers a convenient solutions [72], [73], [74], at the expense of a somewhat more complex receiver structure.

## VIII. System Performance Analysis

### A. Assumptions

Having discussed the network architecture and its nano, intrabody, and body-area networks, in this section we analyze the performance of the whole system. We assume a

TABLE II
SYSTEM PARAMETERS USED FOR THE ANALYSIS

| Parameter | Value |
|---|---|
| **Nano-network:** | |
| Nano-nodes concentration | 10-200 per $cm^3$ |
| Frequency band | 0.1-10 THz |
| Transmission rate | 1 Mbit/s |
| Max. Tx power | 0 dBm |
| Pulse duration | $10^{-13}$ s |
| Path loss | 130 dB/mm |
| Rx sensitivity | -130 dBm |
| Frame size | 64 B |
| Charging frequency | 1 Hz |
| Battery energy | 19.2 fJ |
| Total blood volume | 4.8 $dm^3$ |
| Blood velocity | 13-16 cm/s |
| **Intra-body network:** | |
| Frequency band | 2.4 GHz |
| Transmission power | -24 dBm |
| Receiver sensitivity | -90 dBm |
| Throughput | 4.8 kbit/s |
| **Body area network:** | |
| Frequency band | 2.4 GHz |
| Transmission power | -5 dBm |
| Receiver sensitivity | -82 dBm |
| Throughput | 125 kbit/s |

viewpoint of medical doctors who deal with pulmonary circulation disorders and would like to use the system to detect an artery occlusion, i.e., a situation when an artery is blocked for blood flow. We assume $N = 20$ bio-sensors located in pulmonary arteries and continuously transmitting beacon signals with their ID. Nano-nodes, flowing nearby, wirelessly collect frames from bio-sensors and forward them to the gateway node, frames being further sent to the subcutaneous node and eventually reach the wearable device (e.g., a smartphone). Finally, a medical doctor can check the data and if no frame comes from a specific bio-sensor, an artery occlusion can be suspected, and the doctor can initiate the second stage of system activity, by sending a request to a bio-actuator in a pulmonary artery to release medicines helping to remove the occlusion and restore the correct blood flow. The request frame should travel a similar way back through the whole system: from the wearable device to the subcutaneous node, then to the nano-gateway, and finally via nano-nodes to the chosen bio-actuator.

Having this in mind, the system performance analysis is focused on studying how quickly the system can react, depending on the concentration of the nano-nodes in the blood. We calculate the reaction times in both stages of the system operation: 1) how quickly the doctor can get the information about the occlusion after it happens and 2) how quickly a bio-actuator can be triggered after the doctor sends a request.

The parameters for the analysis are shown in Table II. The concentration of nano-nodes in the blood varies from 10 to 200 per $cm^3$, the other parameters being based on earlier studies in this topic, assuming communication in the THz band with the transmission rate of 1 Mbit/s [40]. Taking the propagation environment into account, which is blood, the communication range is assumed to be approximately 1 mm [38], the size of the frame is 64 B and the charging

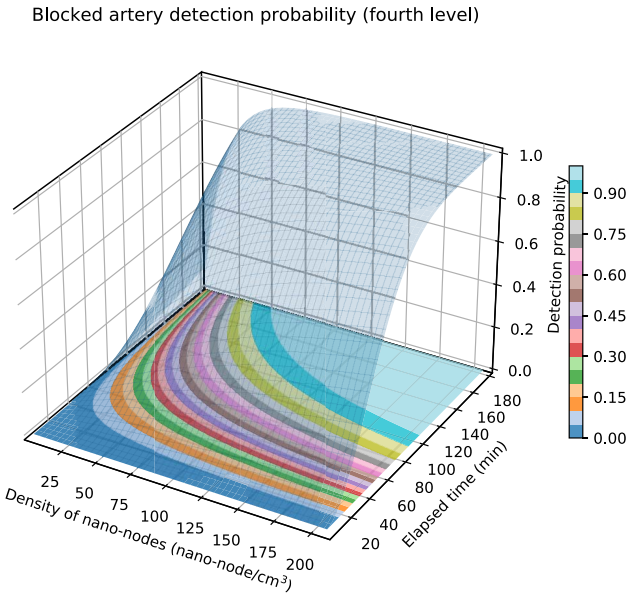


Fig. 4. Probability of frame delivery from a bio-sensor via the nano-network.

frequency is 1 Hz [75]. For the intra- and off-body systems parts, which both work at the 2.4-GHz band, the transmission power, receiving sensitivity, and the throughput are also given in Table II.

As results demonstrate, the bottleneck of the whole system lies in its nano-network part, which is expected considering the very limited communication range of nano-nodes (in the order of millimeters) comparing with the length and volume of the human bloodstream, thus, the analysis is about the nano-network mainly. For the intra- and body-area parts, we focus on link budgets proving that the system is working reliably and with delay orders of magnitude lower than those for the nano-network.

### B. Nano-Network

Both stages of system activity are analyzed. First, the scenario of gathering data frames from bio-sensors is considered in Fig. 4: given the concentration of nano-nodes in the blood and the elapsed time, we calculate the probability $p_Q$ that the nano-network delivers a frame from a specific bio-sensor in the elapsed time $t$. Frames are also kept no longer that $t$ min in the nano-nodes memory, so $p_Q$ can be interpreted as the probability of detection of the artery occlusion (if it happened) in the last $2t$ min. Taking a concentration of 100 nano-nodes per $cm^3$ in 1 h, the probability is around 45% increasing to 78% in 2 h, while for double concentration, we get around 60% and 97%, respectively; these results show that in a time interval between 1 and 2 h, reasonable results are obtained, 3 h being enough for an operation of the system with a very high probability for medical purposes.

Another view on system performance is presented in Fig. 5, where the probability of receiving a frame from a specific bio-sensor is given, assuming that nano-nodes keep frames in memory by $\tau$ min. Taking again 1 and 2 h, we get a probability around 63% and 87% for 1-h memory and 87% and 97% for 2 h, respectively, reinforcing the idea that the time

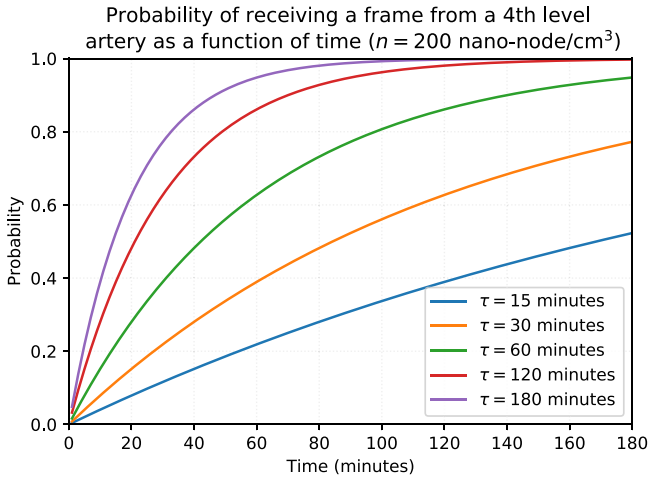


Fig. 5. Probability of receiving a frame from a bio-sensor as a function of time.

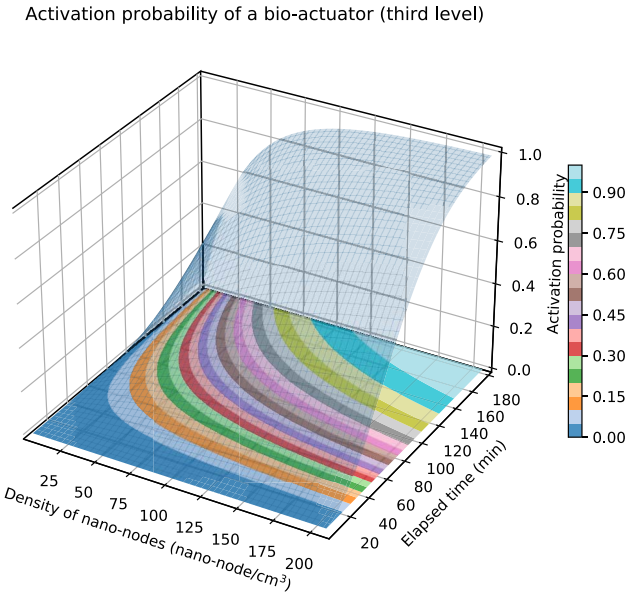


Fig. 6. Probability of activating a bio-actuator.

interval between 1 and 2 h seems to be enable a good choice for system performance, 3-h leading once more to a very high probability. This is a view that a medical doctor or the patient himself could have: the frames from each bio-sensor should be observed in time $T$ with the given probability. If the probability is very high and no frames are observed, it is a clear indication that an occlusion is highly probable and an alarm should be triggered.

The second stage of system activity is related to the scenario when a medical doctor would like to activate a bio-actuator, e.g., after discovering the artery blockage. The results in Fig. 6 present the probability of activation of a chosen bio-actuator in the elapsed time of $t$ min. As this probability depends of the average nano-node concentration and the bio-actuator coverage zone volume, it is the same for bio-actuators at 1st, 2nd, and 3rd levels. Taking again a concentration of 100 nano-nodes per cm$^3$ in 1 h, the probability is around 25%, increasing to 50% in 2 h, while for double concentration, we get around 37% and 73%, respectively; we can conclude that if the whole system is designed to enable a medical reaction for an occlusion in a few hours, the concentration of nano-nodes in the blood should be at least 150 per cm$^3$.

### C. Intrabody Network

In the case of the intrabody link between the nano-gateway (implanted at a depth of around 4 cm) and the subcutaneous node, a preliminary analysis can be performed with the aid of previously accomplished phantom-based measurements. For the sake of simplicity, only the most relevant details are summarized in this section. A complete description of the measurement campaigns can be found in [76] and [77].

In [76], two different setups were configured: 1) heart muscle phantom and 2) heart muscle and fat phantoms. It should be noted that although experiments in [76] were designed for heart tissue, blood and heart have nearly the same dielectric properties, so that the subsequent liquid phantom formulation is nearly identical. For both configurations, phantoms were poured into a squared plastic container whose size is $25 \times 25 \times 25$ cm$^3$ in order to replicate the human chest.

TABLE III
PATH LOSS MODELS IN THE CHEST AREA FOR ISM BAND FROM PHANTOM MEASUREMENTS

| | **Heart muscle** | **Heart muscle + fat** |
|---|---|---|
| $L_0$[dB] | 22.92 | 21.85 |
| $\alpha_{log}$ | 4.12 | 4.12 |
| $\sigma$[dB] | 7.3 | 4.5 |

The transmitting antenna was immersed into a liquid phantom that aims to replicate the dielectric properties of the heart/blood. The receiving antenna was located on the inner wall of either the heart phantom layer, or the fat phantom layer, thus, the subcutaneous receiver was emulated.

The implantable antenna was a conformable meander antenna [45], whose location was controlled automatically by using a 3-D cartesian positioner. On the contrary, the subcutaneous antenna [45] was fixed at the internal wall of the phantom container and it was designed as a rigid patch antenna.

Considering the two configurations aforementioned, it was found that the path loss was well fitted by the typical log-distance model

$$L_{p\ [\mathrm{dB}]} = L_{0\ [\mathrm{dB}]} + 10\,\alpha_{\log}\log(d/d_0) + N\big(0, \sigma_{[\mathrm{dB}]}\big) \quad (28)$$

where $L_0$ is the path loss at the reference distance $d_0$, which is taken as 4 cm, $\alpha_{\log}$ is the average power decay, and $N(0, \sigma)$ is the Normal Distribution, with zero mean and standard deviation $\sigma$. Models are almost identical regardless of considering fat or not, as it can be seen in Table III, which is due to the fact that the fat layer only adds extra loss but does not modify the trend of loss with distance [78]. For both cases, path loss for a distance of 4-cm between the implanted transmitter and the subcutaneous receiver is around 22 dB, which means that communications in 2.4-GHz between the superior vena cava and the surface of the body will be easily feasible. For the sake of comparison, if the UWB band would considered,

the link loss for 4 cm is more than twice than the one for the previous frequency (54.2 dB). This would lead to a more complex scenario where much higher losses should be compensated for, managing a successful communication between the nano-gateway and the exterior of the body.

Regarding link performance, an output power of −24 dBm [79], regardless of the modulation scheme, is enough to achieve an acceptable bit error rate in this kind of devices. On the other hand, during experiments, the receiver's sensitivity was measured to be −90 dBm [76]. Considering 22 to 23 dB of path loss for 1- or 2-layer configurations, respectively, the link budget reveals a really feasible communication for the intrabody link. The throughput for this link is 4.8 kbit/s, as it can be also obtained from [79] where the same equipment is used. Considering the data coming from the nano-network, the gateway should be able to send packets containing a number of frames coming from each bio-sensor (an integer number, 32 bits) for 20 bio-sensors, once per second, which is only 640 bit/s. We can then conclude that the available throughput is more than the one required for this medical application.

### D. Body Area and External Networks

As mentioned before, the off-body connection between the wearable device and the external network can be easily implemented via WiFi or a cellular system, hence, being well-known and easily characterized, without imposing any limitations to the overall system.

Assuming that the on-body connection is implemented in Bluetooth LE, the data rate is more than enough to satisfy the application requirements, even if just half of its maximum is taken due to the TDD mode. The power difference (between transmitter and receiver) is 77 dB (Table II), which seems to be enough to accommodate the system loss in this link (the brief literature survey reported above shows losses that are lower than this power difference).

In conclusion, a careful system design for the on- and off-body links seems to be capable of accommodating the overall system requirements, hence, not being the key constraint for the implementation of this overall system.

## IX. Technology Readiness Discussion

In this article, a global architecture for the proposed diagnostic system is described and analyzed with the derived mathematical model. It is, however, worthwhile, to consider the feasibility of constructing such a system in practice, having in mind the current state of the respective technologies. Here, two parts of the system should be considered separately: 1) THz-communicating nodes (nano-nodes mainly) and 2) BAN devices.

Nano-nodes are not expected to perform complex computing operations. The current technology already makes it possible to integrate all the hardware elements in a few micrometers to implement the desired functionalities, as described in [34]. Regarding energy harvesting and storage, the charging and storage system is based on the use of zinc oxide capacitors and nano-wires. This technology exists for about two decades, so its implementation in nano-devices is perfectly possible [80], [81]. However, technological limits concern the communication capabilities of these nodes. The communication system is limited, first of all, by the size of the nano-devices (less than $100\mu$ m$^2$); at this scale, the operating frequencies are in the THz range and the only plausible technology would be the use of graphene-based antennas. For several years, important advances have been made in the use of graphene antennas in biomedical applications [82], [83]. Yet, this technology is not mature for integration into nano-devices, due to the need for optical pumping in transmission and reception; although optical pumping solves the communication problems with graphene antennas, their size is still several orders of magnitude larger than that of nano-devices and further research is needed to reduce their size [84]. These technology limitations concern also other nodes: bio-sensors/actuators and the nano-gateway, but only their THz-communicating interfaces.

On the other hand, the technology for implanting medical nodes at the millimeter scale is clearly more advanced. Looking for an existing technology that could be applied in the proposed system for PE, the artificial pacemaker seems to be the most relevant one [85]. The functions of such a device are quite similar to the proposed subcutaneous node with its own power source. Even more suitable is another, recently developed technology: a leadless pacemaker [86], where the whole device is implanted inside the cardiovascular system, like the proposed nano-gateway. Communication between such devices inside the body, using GHz interfaces, has also been already validated by in-vivo experiments based on phantoms and animals [45], [51].

The devices releasing medications are also already present in everyday practice: insulin pumps with or without continuous glucose monitoring [87] are even more advanced than the requirements of the system presented in this article. Insulin pumps release drugs continuously with different doses depending on the glucose concentration, whereas in the case of embolism, considered in this article, there is just a single predefined drug dose released.

## X. Conclusion

We have proposed a new diagnostic system based on implanted devices and nano-nodes circulating in the cardiovascular system. The system consists of bio-sensors and bio-actuators located in the pulmonary arteries, and a network of nano-nodes carried by the blood flow. A gateway node in the superior vena cava and a subcutaneous node connected to a wearable device are responsible for transferring information out of the body and vice versa. The system elements communicate at THz band in its nano-network part and at GHz between the nano-gateway and the subcutaneous node transmitting to a wearable device, like a smartphone. The whole system enables two-way communications: 1) from the bio-sensors reporting about possible cardiovascular issues to the external devices and 2) reversely, from the medical staff to the internal bio-actuators, e.g., ordering the release of specific drugs. The proposed solution does not require a patient to

TABLE IV
LIST OF ALL VARIABLES USED IN THE MODEL

| Var. | Description |
|---|---|
| $D_{cyl}$ | Flow diameter [m]. |
| $d$ | Distance [m]. |
| $d_0$ | Reference distance [m]. |
| $d_{mm}$ | Radius of the gateway coverage zone [m]. |
| $d_{nn}$ | Distance travelled by the nano-node [m]. |
| $E_{b=0}$ | Energy required to transmit or receive a 0 bit symbol [J]. |
| $E_{b=1}$ | Energy required to transmit or receive a 1 bit symbol [J]. |
| $E_{f,max}$ | Maximum energy required to transmit or receive a frame [J]. |
| $f_{cha}(t)$ | Nano-node charging frequency as a function of time [Hz]. |
| $\overline{f_{cha}}$ | Average nano-node charging frequency [Hz]. |
| $L_p$ | Path Loss [dB]. |
| $L_0$ | Path Loss at reference distance [dB]. |
| $N$ | Number of uniformly distributed nano-nodes in the flow-guided nano-network. |
| $N_\theta$ | Number of nano-nodes that maximizes throughput. |
| $p_{a,m}$ | Probability of successfully activating a nano-actuator in round $m$. |
| $p_{cv}$ | Probability of a nano-node being in the coverage zone of a nano-gateway or of a bio-sensor/actuator. |
| $p_{cx}$ | Probability of a nano-node being in the collision zone. |
| $p_{d,\tau,\epsilon}$ | Probability of the nano-gateway receiving a frame before $\epsilon$ time units if a nano-node remembers a bio-sensor frame reception for $\tau$ time units. |
| $p_f$ | Probability of not detecting a bio-sensor in a time slot. |
| $p_{f,\tau}$ | Probability of not detecting a bio-sensor after $\tau$ time slots. |
| $p_{Q,a}$ | Probability of a bio-actuator getting activated. |
| $p_{Q,d}$ | Probability of no false blocked artery detection being performed. |
| $p_{rx,T}$ | Probability of a nano-node receiving a frame from a bio-sensor in a round. |
| $p_{rx,T,\tau}$ | Probability of a nano-node receiving at least one frame from a bio-sensor after $\tau$ rounds. |
| $p_{tx}$ | Probability of a nano-node being in the transmission zone. |
| $P_{rx\ min}$ | Nano-gateway receiver sensitivity [W]. |
| $P_{tx}$ | Nano-node transmission power [W]. |
| $Q$ | Energy that can be stored by a nano-node [J]. |
| $R$ | Nano-node transmission rate [bit/s]. |
| $\overline{r_{T,av}}$ | Average number of successful frames by the nano-nodes during a round. |
| $T_{cha}(t)$ | Time required by a nano-node to complete a round in the flow-guided network [s]. |
| $\overline{T_{cir}}$ | Average time required by a nano-node to complete a round in the flow-guided network [s]. |
| $t_f$ | Time required to transmit a frame [s]. |
| $t_p$ | Duration of the electromagnetic pulses in the On-Off Keying modulation [s]. |
| $\overline{v}$ | Average speed of the nano-node in the nano-gateway, bio-sensor, or bio-actuator coverage zone [m/s]. |
| $V_{cv}$ | Volume of the nano-gateway, bio-sensor, or bio-actuator coverage zone [$m^3$]. |
| $V_{cx}$ | Volume of the nano-gateway collision zone [$m^3$]. |
| $V_{net}$ | Volume of the flow-guided nano-network [$m^3$]. |
| $V_{rx}$ | Volume of the bio-sensor reception zone [$m^3$]. |
| $V_{tx}$ | Volume of the nano-gateway transmission zone [$m^3$]. |
| $\alpha_{lin}$ | Channel path loss linear coefficient [dB/m]. |
| $\alpha_{log}$ | Channel path loss log coefficient. |
| $\phi$ | Number of rounds for activation of the bio-actuator. |
| $\lambda_d$ | Size of the frame data payload [B]. |
| $\lambda_f$ | Size of the frame [B]. |
| $\lambda_h$ | Size of the frame header addressing field [B]. |
| $\lambda_o$ | Size of other fields the frame [B]. |
| $\sigma$ | Standard deviation. |
| $\theta$ | Flow-guided nano-network throughput [bit/s]. |

be hospitalized, on the contrary, it can be used by a person leading normal active life.

In this article, we have focused on medical applications related to diseases of the vascular circulation system, which are one of the main causes of deaths in developed countries. We have addressed the issue of pulmonary blood circulation disorders, which can remain unnoticed by several days, at the same time being life threatening conditions. The delay in diagnosis of such disorders is known to be an important risk factor of fatal outcome.

Consequently, the performance of our proposed system has been evaluated in terms of diagnosis time and also the time of making a remote medical action, i.e., releasing specific drugs by bio-actuators. The values obtained from our analysis, about 3 h for the diagnosis (for 3rd level artery blockage, and shorter in case of 2nd or 1st level occlusion) and another 3 h for releasing drugs without patient hospitalization, are very promising comparing with current practice and people with high risk of pulmonary disorders could strongly benefit from the presented solution.

While we have focused here on pulmonary disorders, the applications of the presented diagnostic system are not limited only to these problems. There are many other issues related to human vascular system, like tumor, bacterial and viral infections, sepsis and others, and in all these cases medicine can benefit from such a two-way communication system based on BANs and nano-networks providing tools for quick diagnosis and swift medical reaction.

## ANNEX

A summary of all variables used in this article together with their units is given in Table IV.

## REFERENCES


[1] "Google glass." Accessed: Nov. 3, 2021. [Online]. Available: https://www.google.com/glass/start

[2] "Ray-Ban." Accessed: Nov. 3, 2021. [Online]. Available: https://www.ray-ban.com/usa/discover-ray-ban-stories/clp

[3] M. Patel and J. Wang, "Applications, challenges, and prospective in emerging body area networking technologies," *IEEE Wireless Commun.*, vol. 17, no. 1, pp. 80–88, Feb. 2010.

[4] Y. A. Qadri, A. Nauman, Y. B. Zikria, A. V. Vasilakos, and S. W. Kim, "The future of Healthcare Internet of Things: A survey of emerging technologies," *IEEE Commun. Surveys Tuts.*, vol. 22, no. 2, pp. 1121–1167, 2nd Quart., 2020.

[5] P. Kulakowski, K. Turbic, and L. M. Correia, "From nano-communications to body area networks: A perspective on truly personal communications," *IEEE Access*, vol. 8, pp. 159839–159853, 2020.

[6] F. Dressler and S. Fischer, "Connecting in-body nano communication with body area networks: Challenges and opportunities of the Internet of Nano Things," *Nano Commun. Netw.*, vol. 6, no. 2, pp. 29–38, 2015.

[7] H. Rahmani and A. Babakhani, "A 1.6mm$^3$ wirelessly powered reconfigurable FDD radio with on-chip antennas achieving 4.7 pJ/b TX and 1 pJ/b RX energy efficiencies for medical implants," in *Proc. IEEE Custom Integr. Circuits Conf. (CICC)*, 2020, pp. 1–4.

[8] B. Jamali, S. Razavian, and A. Babakhani, "Fully electronic silicon-based THz pulse sources and detectors," in *Proc. Terahertz Photon.*, 2020, pp. 41–48.

[9] "Causes and occurrence of deaths in the EU." Eurostat. 2020. Accessed: Oct. 7, 2021. [Online]. Available: https://ec.europa.eu/eurostat/web/products-eurostat-news/-/ddn-20200721-1

[10] I. F. Akyildiz, M. Ghovanloo, U. Guler, T. Ozkaya-Ahmadov, A. F. Sarioglu, and B. D. Unluturk, "PANACEA: An Internet of bio-NanoThings application for early detection and mitigation of infectious diseases," *IEEE Access*, vol. 8, pp. 140512–140523, 2020.

[11] H. Habibzadeh, K. Dinesh, O. R. Shishvan, A. Boggio-Dandry, G. Sharma, and T. Soyata, "A survey of Healthcare Internet of Things (HIoT): A clinical perspective," *IEEE Internet Things J.*, vol. 7, no. 1, pp. 53–71, Jan. 2020.

[12] F. Alshehri and G. Muhammad, "A comprehensive survey of the Internet of Things (IoT) and AI-based smart healthcare," *IEEE Access*, vol. 9, pp. 3660–3678, 2021.

[13] Y.-S. Su, T.-J. Ding, and M.-Y. Chen, "Deep learning methods in Internet of Medical Things for valvular heart disease screening system," *IEEE Internet Things J.*, vol. 8, no. 23, pp. 16921–16932, Dec. 2021.

[14] L. Sun, X. Jiang, H. Ren, and Y. Guo, "Edge-cloud computing and artificial intelligence in Internet of Medical Things: Architecture, technology and application," *IEEE Access*, vol. 8, pp. 101079–101092, 2020.

[15] W. J. Powers et al., "Guidelines for the early management of patients with acute ischemic stroke: 2019 update to the 2018 guidelines for the early management of acute ischemic stroke: A guideline for healthcare professionals from the American heart association/American stroke association," *Stroke*, vol. 50, no. 12, pp. e344–e418, 2019.

[16] S. V. Konstantinides et al., "2019 ESC guidelines for the diagnosis and management of acute pulmonary embolism developed in collaboration with the European respiratory society (ERS): The task force for the diagnosis and management of acute pulmonary embolism of the European society of cardiology (ESC)," *Eur. Heart J.*, vol. 41, no. 4, pp. 543–603, Aug. 2019.

[17] J.-P. Collet et al., "2020 ESC guidelines for the management of acute coronary syndromes in patients presenting without persistent ST-segment elevation: The task force for the management of acute coronary syndromes in patients presenting without persistent ST-segment elevation of the European society of cardiology (ESC)," *Eur. Heart J.*, vol. 42, p. 2298, Jun. 2021.

[18] M. Arrigo and L. C. Huber, "Pulmonary embolism and heart failure: A reappraisal," *Cardiac Failure Rev.*, vol. 7, p. e03, Feb. 2021.

[19] D. Siegal and W. Lim, "Chapter 142—Venous thromboembolism," in *Hematology*, 7th ed., R. Hoffman et al., Eds. Amsterdam, The Netherlands: Elsevier, 2018, pp. 2102–2112.

[20] D. R. Anderson and D. C. Barnes, "Computerized tomographic pulmonary angiography versus ventilation perfusion lung scanning for the diagnosis of pulmonary embolism," *Current Opinion Pulmonary Med.*, vol. 15, no. 5, pp. 425–429, Sep. 2009.

[21] K. R. Nilsson, J. P. Piccini, and M. D. C. Llc, *The Osler Medical Handbook*. Philadelphia, PA, USA: Mosby, 2006.

[22] C. Wittram, A. C. Waltman, J.-A. O. Shepard, E. Halpern, and L. R. Goodman, "Discordance between CT and angiography in the PIOPED II study," *Radiology*, vol. 244, no. 3, pp. 883–889, Sep. 2007.

[23] P. D. Stein, "Gadolinium-enhanced magnetic resonance angiography for pulmonary embolism," *Ann. Internal Med.*, vol. 152, no. 7, p. 434, Apr. 2010.

[24] S. Walen, R. A. Damoiseaux, S. M. Uil, and J. W. van den Berg, "Diagnostic delay of pulmonary embolism in primary and secondary care: A retrospective cohort study," *Brit. J. General Pract.*, vol. 66, no. 647, pp. e444–e450, 2016.

[25] Y. Bulbul, S. Ozsu, P. Kosucu, F. Oztuna, T. Ozlu, and M. Topbas, "Time delay between onset of symptoms and diagnosis in pulmonary thromboembolism," *Respiration*, vol. 78, no. 1, pp. 36–41, 2009.

[26] C. G. Elliott, S. Z. Goldhaber, and R. L. Jensen, "Delays in diagnosis of deep vein thrombosis and pulmonary embolism," *Chest*, vol. 128, no. 5, pp. 3372–3376, Nov. 2005.

[27] A. G. Bach et al., "Timing of pulmonary embolism diagnosis in the emergency department," *Thrombosis Res.*, vol. 137, pp. 53–57, Jan. 2016.

[28] B. Ibanez et al., "2017 ESC guidelines for the management of acute myocardial infarction in patients presenting with ST-segment elevation: The task force for the management of acute myocardial infarction in patients presenting with ST-segment elevation of the European society of cardiology (ESC)," *Eur. Heart J.*, vol. 39, no. 2, pp. 119–177, Aug. 2017.

[29] C. Caro, *The Mechanics of the Circulation*. Cambridge, U.K.: Cambridge Univ. Press, 2011.

[30] J. E. Zablah and G. J. Morgan, "Pulmonary artery stenting," *Interv. Cardiol. Clin.*, vol. 8, no. 1, pp. 33–46, Jan. 2019.

[31] S. Hassan, M. N. Ali, and B. Ghafoor, "Evolutionary perspective of drug eluting stents: From thick polymer to polymer free approach," *J. Cardiothoracic Surg.*, vol. 17, no. 1, p. 65, Apr. 2022.

[32] C. Stone, *Current Diagnosis & Treatment*. New York, NY, USA: McGraw-Hill Educ., 2017.

[33] A. S. Ferrell, Y. J. Zhang, O. Diaz, R. Klucznik, and G. W. Britz, "Modern interventional management of stroke," *Methodist DeBakey Cardiovasc. J.*, vol. 10, no. 2, pp. 105–110, Apr. 2014.

[34] S. Canovas-Carrasco, A.-J. Garcia-Sanchez, F. Garcia-Sanchez, and J. Garcia-Haro, "Conceptual design of a nano-networking device," *Sensors*, vol. 16, no. 12, p. 2104, Dec. 2016.

[35] R. Asorey-Cacheda, S. Canovas-Carrasco, A.-J. Garcia-Sanchez, and J. Garcia-Haro, "An analytical approach to flow-guided nanocommunication networks," *Sensors*, vol. 20, no. 5, p. 1332, Feb. 2020.

[36] S. Canovas-Carrasco, A.-J. Garcia-Sanchez, and J. Garcia-Haro, "A nanoscale communication network scheme and energy model for a human hand scenario," *Nano Commun. Netw.*, vol. 15, pp. 17–27, Mar. 2018.

[37] K. Y. R. Kam, J. M. Mari, and T. J. Wigmore, "Adjacent central venous catheters can result in immediate aspiration of infused drugs during renal replacement therapy," *Anaesthesia*, vol. 67, no. 2, pp. 115–121, Nov. 2011.

[38] S. Canovas-Carrasco, A.-J. Garcia-Sanchez, and J. Garcia-Haro, "On the nature of energy-feasible wireless nanosensor networks," *Sensors*, vol. 18, no. 5, p. 1356, Apr. 2018.

[39] J. M. Jornet and I. F. Akyildiz, "Femtosecond-long pulse-based modulation for terahertz band communication in nanonetworks," *IEEE Trans. Commun.*, vol. 62, no. 5, pp. 1742–1754, May 2014.

[40] S. Canovas-Carrasco, R. Asorey-Cacheda, A.-J. Garcia-Sanchez, J. Garcia-Haro, K. Wojcik, and P. Kulakowski, "Understanding the applicability of terahertz flow-guided nano-networks for medical applications," *IEEE Access*, vol. 8, pp. 214224–214239, 2020.

[41] R. Alsheikh, N. Akkari, and E. Fadel, "MAC protocols for wireless nano-sensor networks: Performance analysis and design guidelines," in *Proc. 6th Int. Conf. Digit. Inf. Process. Commun. (ICDIPC)*, 2016, pp. 129–134.

[42] J. M. Jornet, J. C. Pujol, and J. S. Pareta, "PHLAME: A physical layer aware MAC protocol for electromagnetic nanonetworks in the terahertz band," *Nano Commun. Netw.*, vol. 3, no. 1, pp. 74–81, 2012.

[43] Q. Xia, Z. Hossain, M. J. Medley, and J. M. Jornet, "A link-layer synchronization and medium access control protocol for terahertz-band communication networks," *IEEE Trans. Mobile Comput.*, vol. 20, no. 1, pp. 2–18, Jan. 2021.

[44] R. Chavez-Santiago et al., "Experimental path loss models for in-body communications within 2.36-2.5 GHz," *IEEE J. Biomed. Health Inform.*, vol. 19, no. 3, pp. 930–937, May 2015.

[45] P. Bose, A. Khaleghi, M. Albatat, J. Bergsland, and I. Balasingham, "RF channel modeling for implant-to-implant communication and implant to subcutaneous implant communication for future leadless cardiac pacemakers," *IEEE Trans. Biomed. Eng.*, vol. 65, no. 12, pp. 2798–2807, Dec. 2018.

[46] R. Chávez-Santiago, I. Balasingham, and J. Bergsland, "Ultrawideband technology in medicine: A survey," *J. Elect. Comput. Eng.*, vol. 2012, Apr. 2012, Art. no. 716973.

[47] R. Chávez-Santiago, C. García-Pardo, A. Fornes-Leal, A. Vallés-Lluch, I. Balasingham, and N. Cardona, "Ultra wideband propagation for future in-body sensor networks," in *Proc. IEEE 25th Annu. Int. Symp. Pers. Indoor Mobile Radio Commun. (PIMRC)*, 2014, pp. 2160–2163.

[48] C. Garcia-Pardo et al., "Experimental ultra wideband path loss models for implant communications," in *Proc. IEEE 27th Annu. Int. Symp. Pers. Indoor Mobile Radio Commun. (PIMRC)*, Valencia, Spain, Sep. 2016, pp. 1–6.

[49] C. Garcia-Pardo et al., "Ultrawideband technology for medical in-body sensor networks: An overview of the human body as a propagation medium, phantoms, and approaches for propagation analysis," *IEEE Antennas Propag. Mag.*, vol. 60, no. 3, pp. 19–33, Jun. 2018.

[50] C. Andreu, C. Garcia-Pardo, A. Fomes-Leal, M. Cabedo-Fabrés, and N. Cardona, "UWB in-body channel performance by using a direct antenna designing procedure," in *Proc. 11th Eur. Conf. Antennas Propag. (EUCAP)*, 2017, pp. 278–282.

[51] P. Bose, A. Khaleghi, and I. Balasingham, "In-body and off-body channel modeling for future leadless cardiac pacemakers based on phantom and animal experiments," *IEEE Antennas Wireless Propag. Lett.*, vol. 17, pp. 2484–2488, 2018.

[52] L.-J. Xu, Y.-X. Guo, and W. Wu, "Dual-band implantable antenna with open-end slots on ground," *IEEE Antennas Wireless Propag. Lett.*, vol. 11, pp. 1564–1567, 2012.

[53] F. Faisal, M. Zada, A. Ejaz, Y. Amin, S. Ullah, and H. Yoo, "A miniaturized dual-band implantable antenna system for medical applications," *IEEE Trans. Antennas Propag.*, vol. 68, no. 2, pp. 1161–1165, Feb. 2020.

[54] J. Blauert, Y.-S. Kang, and A. Kiourti, "In vivo testing of a miniature 2.4/4.8 GHz implantable antenna in postmortem human subject," *IEEE Antennas Wireless Propag. Lett.*, vol. 17, pp. 2334–2338, 2018.

[55] E. Motovilova and S. Y. Huang, "A review on reconfigurable liquid dielectric antennas," *Materials*, vol. 13, no. 8, p. 1863, Apr. 2020.

[56] S. G. Kirtania et al., "Flexible antennas: A review," *Micromachines*, vol. 11, no. 9, p. 847, 2020.

[57] N. Tiercelin, P. Coquet, R. Sauleau, V. Senez, and H. Fujita, "Polydimethylsiloxane membranes for millimeter-wave planar ultra flexible antennas," *J. Micromech. Microeng.*, vol. 16, no. 11, pp. 2389–2395, Nov. 2006.

[58] C. W. Kim and T. S. P. See, "RF transmission power loss variation with abdominal tissues thicknesses for ingestible source," in *Proc. IEEE 13th Int. Conf. e-Health Netw. Appl. Services.*, 2011, pp. 282–287.

[59] M. F. Awan et al., "Experimental phantom-based evaluation of physical layer security for future leadless cardiac pacemaker," in *Proc. IEEE 29th Annu. Int. Symp. Pers. Indoor Mobile Radio Commun. (PIMRC)*, 2018, pp. 333–339.

[60] J. Blauert and A. Kiourti, "Bio-matched horn: A novel 1–9 GHz on-body antenna for low-loss biomedical telemetry with implants," *IEEE Trans. Antennas Propag.*, vol. 67, no. 8, pp. 5054–5062, Aug. 2019.

[61] R. B. Green, M. Hays, M. Mangino, and E. Topsakal, "An anatomical model for the simulation and development of subcutaneous implantable wireless devices," *IEEE Trans. Antennas Propag.*, vol. 68, no. 10, pp. 7170–7178, Oct. 2020.

[62] *IEEE Standard for Local and Metropolitan Area Networks—Part 15.6: Wireless Body Area Networks*, IEEE Standard 802.15.6-2012, Feb. 2012.

[63] S. L. Cotton, "A statistical model for shadowed body-centric communications channels: Theory and validation," *IEEE Trans. Antennas Propag.*, vol. 62, no. 3, pp. 1416–1424, Mar. 2014.

[64] K. Turbic and L. M. Correia, "Effects on polarization characteristics of off-body channels with dynamic users," in *Proc. IEEE Wireless Commun. Netw. Conf. (WCNC)*, Seoul, South Korea, Apr. 2020, pp. 1–6.

[65] S. L. Cotton, R. D'Errico, and C. Oestges, "A review of radio channel models for body centric communications," *Radio Sci.*, vol. 49, no. 6, pp. 371–388, Jun. 2014.

[66] G. Koutitas, "Multiple human effects in body area networks," *IEEE Antennas Wireless Propag. Lett.*, vol. 9, pp. 938–941, 2010.

[67] T. Mavridis, L. Petrillo, J. Sarrazin, D. Lautru, A. Benlarbi-Delai, and P. De Doncker, "Theoretical and experimental investigation of a 60-GHz off-body propagation model," *IEEE Trans. Antennas Propag.*, vol. 62, no. 1, pp. 393–402, Jan. 2014.

[68] K. Turbic, L. M. Correia, and M. Beko, "A channel model for polarized off-body communications with dynamic users," *IEEE Trans. Antennas Propag.*, vol. 67, no. 11, pp. 7001–7013, Nov. 2019.

[69] S.-C. Kwon, G. Stüber, A. Lopez, and J. Papapolymerou, "Geometrically based statistical model for polarized body-area-network channels," *IEEE Trans. Veh. Technol.*, vol. 62, no. 8, pp. 3518–3530, Oct. 2013.

[70] S.-C. Kwon, G. L. Stüber, A. López, and J. Papapolymerou, "Polarized channel model for body area networks using reflection coefficients," *IEEE Trans. Veh. Technol.*, vol. 64, no. 8, pp. 3822–3828, Aug. 2015.

[71] K. Turbic, M. Särestöniemi, M. Hämäläinen, and L. M. Correia, "User influence on polarization characteristics in off-body channels," *IEEE Access*, vol. 8, pp. 167570–167584, 2020.

[72] L. Vallozzi, P. Van Torre, C. Hertleer, H. Rogier, M. Moeneclaey, and J. Verhaevert, "Wireless communication for Firefighters using dual-polarized textile antennas integrated in their garment," *IEEE Trans. Antennas Propag.*, vol. 58, no. 4, pp. 1357–1368, Apr. 2010.

[73] P. V. Torre, L. Vallozzi, C. Hertleer, H. Rogier, M. Moeneclaey, and J. Verhaevert, "Indoor off-body wireless MIMO communication with dual polarized textile antennas," *IEEE Trans. Antennas Propag.*, vol. 59, no. 2, pp. 631–642, Feb. 2011.

[74] P.-F. Cui, W.-J. Lu, Y. Yu, B. Xue, and H.-B. Zhu, "Off-body spatial diversity reception using circular and linear polarization: Measurement and modeling," *IEEE Commun. Lett.*, vol. 22, no. 1, pp. 209–212, Jan. 2018.

[75] S. Canovas-Carrasco, R. Asorey-Cacheda, A.-J. Garcia-Sanchez, J. Garcia-Haro, P. Kulakowski, and K. Wojcik, "A performance evaluation of an in-body nano-network architecture," in *Proc. IEEE 21st Int. Conf. High Perform. Switch. Routing (HPSR)*, 2020, pp. 1–5.

[76] M. F. Awan, S. Perez-Simbor, C. Garcia-Pardo, K. Kansanen, and N. Cardona, "Experimental phantom-based security analysis for next-generation leadless cardiac pacemakers," *Sensors*, vol. 18, no. 12, p. 4327, Dec. 2018.

[77] S. Castelló-Palacios, C. Garcia-Pardo, A. Fornes-Leal, N. Cardona, and A. Vallés-Lluch, "Full-spectrum phantoms for cm-wave and medical wireless communications," in *Proc. IET Conf. Publ.*, 2018, pp. 1–3.

[78] S. Perez-Simbor, C. Andreu, C. Garcia-Pardo, M. Frasson, and N. Cardona, "UWB path loss models for ingestible devices," *IEEE Trans. Antennas Propag.*, vol. 67, no. 8, pp. 5025–5034, Aug. 2019.

[79] P. Bose, A. Khaleghi, S. Mahmood, M. Albatat, J. Bergsland, and I. Balasingham, "Evaluation of data telemetry for future leadless cardiac pacemaker," *IEEE Access*, vol. 7, pp. 157933–157945, 2019.

[80] H. Xiang, J. Yang, J. Hou, and Q. Zhu, "Piezoelectricity in ZnO nanowires: A first-principles study," *Appl. Phys. Lett.*, vol. 89, no. 22, 2006, Art. no. 223111.

[81] Z. L. Wang and J. Song, "Piezoelectric nanogenerators based on zinc oxide nanowire arrays," *Science*, vol. 312, no. 5771, pp. 242–246, 2006.

[82] G. Varshney, S. Debnath, and A. K. Sharma, "Tunable circularly polarized graphene antenna for THz applications," *Optik*, vol. 223, Dec. 2020, Art. no. 165412.

[83] Y. Tetsu, Y. Kido, M. Hao, S. Takeoka, T. Maruyama, and T. Fujie, "Graphene/Au hybrid antenna coil exfoliated with multi-stacked graphene flakes for ultra-thin biomedical devices," *Adv. Electron. Mater.*, vol. 6, no. 2, 2020, Art. no. 1901143.

[84] Z. Ullah, G. Witjaksono, I. Nawi, N. Tansu, M. I. Khattak, and M. Junaid, "A review on the development of tunable graphene nanoantennas for terahertz optoelectronic and plasmonic applications," *Sensors*, vol. 20, no. 5, p. 1401, 2020. [Online]. Available: https://www.mdpi.com/1424-8220/20/5/1401

[85] G. J. J. Boink, V. M. Christoffels, R. B. Robinson, and H. L. Tan, "The past, present, and future of pacemaker therapies," *Trends Cardiovas. Med.*, vol. 25, no. 8, pp. 661–673, Nov. 2015. [Online]. Available: https://doi.org/10.1016/j.tcm.2015.02.005

[86] G. Mitacchione, M. Schiavone, A. Gasperetti, M. Viecca, A. Curnis, and G. B. Forleo, "Atrioventricular synchronous leadless pacemaker: State of art and broadened indications," *Rev. Cardiovas. Med.*, vol. 22, no. 2, p. 395, 2021. [Online]. Available: https://doi.org/10.31083/j.rcm2202045

[87] R. Nimri, J. Nir, and M. Phillip, "Insulin pump therapy," *Amer. J. Ther.*, vol. 27, no. 1, pp. e30–e41, Jan. 2020. [Online]. Available: https://doi.org/10.1097/mjt.0000000000001097

**Rafael Asorey-cacheda** (Member, IEEE) received his M.Sc. degree in Telecommunication Engineering (major in Telematics and Best Master Thesis Award) and his Ph.D. (cum laude and Best PhD Thesis Award) in Telecommunication Engineering from the Universidade de Vigo, Spain, in 2006 and 2009, respectively. He was a researcher with the Information Technologies Group, University of Vigo, Spain until 2009. Between 2008 and 2009 he was also R&D Manager at Optare Solutions, a Spanish telecommunications company. Between 2009 and 2012, he held an At' ngeles AlvarinŸo position, Xunta de Galicia, Spain. Between 2012 and 2018, he was an associate professor at the Centro Universitario de la Defensa en la Escuela Naval Militar, Universidade de Vigo. Currently, he is an associate professor at the Universidad Politt'ecnica de Cartagena. He is author or coauthor of more than 60 journal and conference papers, mainly in the fields of switching, wireless networking and content distribution. He has been a visiting scholar at New Mexico State University, USA (2007-2011) and at Universidad Politt'ecnica de Cartagena, Spain (2011, 2015). His interests include content distribution, high-performance switching, peer-to-peer networking, wireless networks, and nano-networks.

**Luis M. Correia** (Senior Member, IEEE) was born in Portugal, in 1958. He received the Ph.D. in Electrical and Computer Engineering from IST (Univ. Lisbon) in 1991, where he is currently a Professor in Telecommunications, with his work focused on wireless & mobile communications, with the research activities developed in the INESC-ID institute. He has acted as a consultant for the Portuguese telecommunications operators and regulator, besides other public and private entities, and has been in the Board of Directors of a telecommunications company. He has participated in 32 projects within European frameworks, having coordinated 6 and taken leadership responsibilities at various levels in many others, besides national ones. He has supervised over 230 M.Sc./Ph.D. students, having edited 6 books, contribute to European strategic documents, and authored over 500 papers in international and national journals and conferences, for which served also as a reviewer, editor and board member. Internationally, he was part of 39 Ph.D. juries, and 78 research projects and institutions evaluation committees for funding agencies in 12 countries, and the European Commission and COST. He has been the Chairman of Conference, of the Technical Programme Committee and of the Steering Committee of 25 major conferences, besides other several duties. He was a National Delegate to the COST Domain Committee on ICT. He has launched and served as Chairman of the IEEE Communications Society Portugal Chapter, besides being involved in several other duties in this society at the global level. He is an Honorary Professor of the Gdańsk University of Technology (Poland) and a recipient of the 2021 EurAAP Propagation Award "for leadership in the field of propagation for wireless and mobile communications."

**Concepcion Garcia-Pardo** attended the Universidad Politt'ecnica de Cartagena (UPCT), where she received the Telecommunication Engineering degree in 2007 and the M.Sc. in Information Technologies and Communications in 2008. In 2012, she got her Ph.D. degree with European mention and qualification cum laude, from UPCT, and Ph.D. degree in Microwaves and Microtechnologies with qualification Tr'es Honorable from the Lille 1 University (USTL). Her Ph.D. Thesis was awarded the special prize from UPCT in 2013. In 2012, she joined the Institute of Telecommunications and Multimedia Applications (iTEAM) of the Universitat Polit'ecnica de Valencia (UPV), Spain, where she is currently senior researcher. She is author of more 50 publications of journal and conference papers related to wireless communications. She has also participated in several projects related to wireless communications and wireless medical devices. She was also in the management committee of COST Action CA 15104-IRACON. Her current work is focused on wireless medical devices and wireless communications for body area networks, as well as dielectric characterization of human body tissues.

**Krzysztof Wojcik** received the M.Sc. and Ph.D. degrees in biophysics from Jagiellonian University, Kraków, Poland, in 2003 and 2015, respectively, and the M.D. degree from Jagiellonian University Medical College (JUMC), Kraków, in 2007.

He was an Assistant with the Division of Cell Biophysics Faculty of Biochemistry, Biophysics and Biotechnology, Jagiellonian University, Kraków, from 2007 to 2014. He is an Assistant Professor with the Department of Allergy, Autoimmunity, and Hypercoagulability in II Chair of Internal Medicine JUMC. He is involved in European vasculitis research—FAIRVASC a Horizon 2020 funded project. His research interest is focused on vasculitis and super-resolution microscopy techniques for auto-antibody detection.

**Kenan Turbic** (Member, IEEE) received an MSc degree from the University of Sarajevo in 2011, and a PhD degree (Hons.) in Electrical and Computer Engineering from IST, University of Lisbon, in 2019. He was a postdoctoral research fellow at the INESC-ID research institute, Lisbon, Portugal, and currently he is a postdoctoral researcher at the Chair for Distributed Signal Processing, ICE, RWTH Aachen University, Aachen, Germany. He was actively participating in the COST Action CA15104 (IRACON), to which he contributed with several technical documents and served as one of the Section editors for the final report book. His main research interests include channel modeling and estimation, and signal processing for wireless communications.

**Pawel Kulakowski** received Ph.D. in telecommunications from the AGH University of Science and Technology in Krakow, Poland, in 2007, and currently he is working there as an associate professor. In 2008-2013, he spent over 2 years in total as a post-doc or a visiting professor at Technical University of Cartagena, University of Girona, University of Castilla-La Mancha and University of Seville. He was involved in European research projects, serving in the Management Committees of COST Actions: IC1004, CA15104 IRACON, CA20120 INTERACT, and CA20124 AI4NICU, focusing on topics of nano-networking, AI in neonatology, wireless sensor networks, indoor localization and wireless communications in general. In 2019-2021, he was also an R&D manager for a national research project on 5G network planning. His current research interests include nano-networks and AI applications both in 5/6G mobile systems and in medicine. He was recognized with several scientific distinctions, including three awards for his conference papers and a governmental scholarship for young outstanding researchers.